

Supporting Information

Effective Ion Mobility and Long-Term Dark Current of Metal-Halide Perovskites of Different Crystallinity and Composition

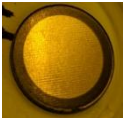
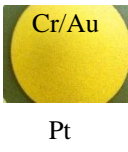



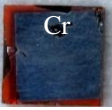
Marisé García-Battle¹, Sarah Deumel², Judith E. Huedler², Sandro F. Tedde², Osbel Almora¹ and Germà Garcia-Belmonte^{1*}

¹ *Institute of Advanced Materials (INAM), Universitat Jaume I, 12006 Castelló, Spain*

² *Siemens Healthineers AG, Technology Excellence, Guenther-Scharowsky-Strasse 1, 91058 Erlangen, Germany*

*Email: garciag@uji.es

17 August 2022

Table S1. Characteristics of the samples studied							
Sample Composition	Number of samples	Cristallinity	Dimensions	Sample thickness (μm)	Electrode configuration and area	Picture of the sample	Picture of the electrodes
MAPbI ₃	6	MC	diameter ~15 mm	~1000	Pt/Cr ~ 1cm ²		
MAPbBr ₃	2	MC	diameter ~15 mm	~1560	Pt/Cr ~ 1cm ²		
MAPbBr ₃	2	SC	3.93 mm × 3.87 mm	~2000	Cr/Cr ~ 0.12 cm ²		

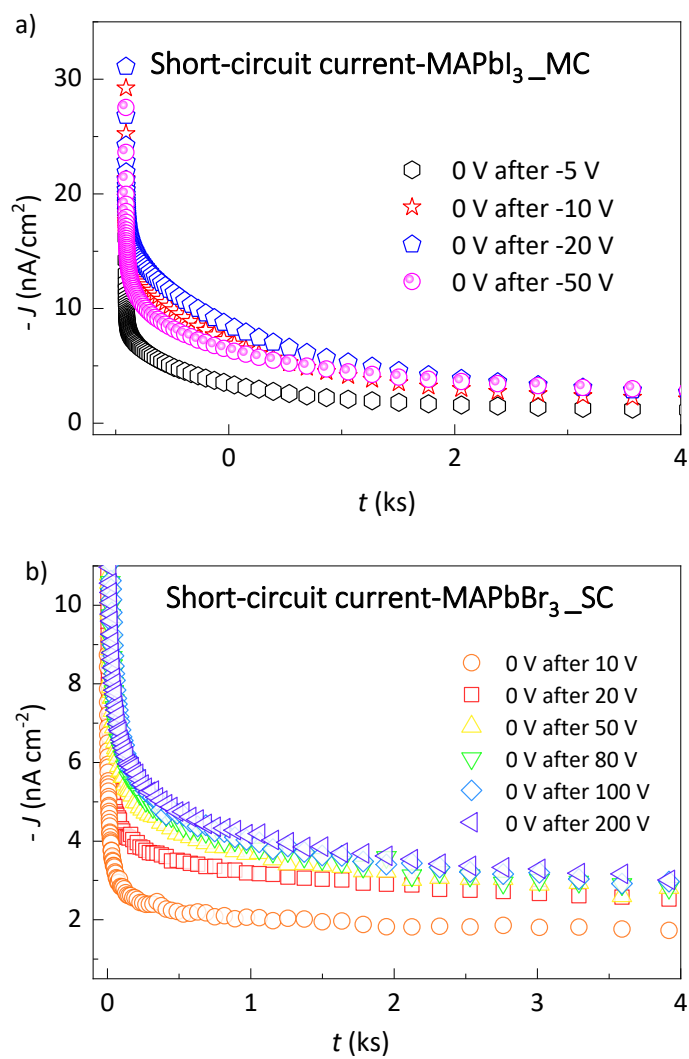


Figure S1 Example on current transient response to short-circuit condition (0 V-bias voltage) of a a) MAPbI₃ MC sample contacted with Pt/Cr electrodes b) a MAPbBr₃ SC symmetrically contacted with evaporated Cr electrodes. Short circuit current

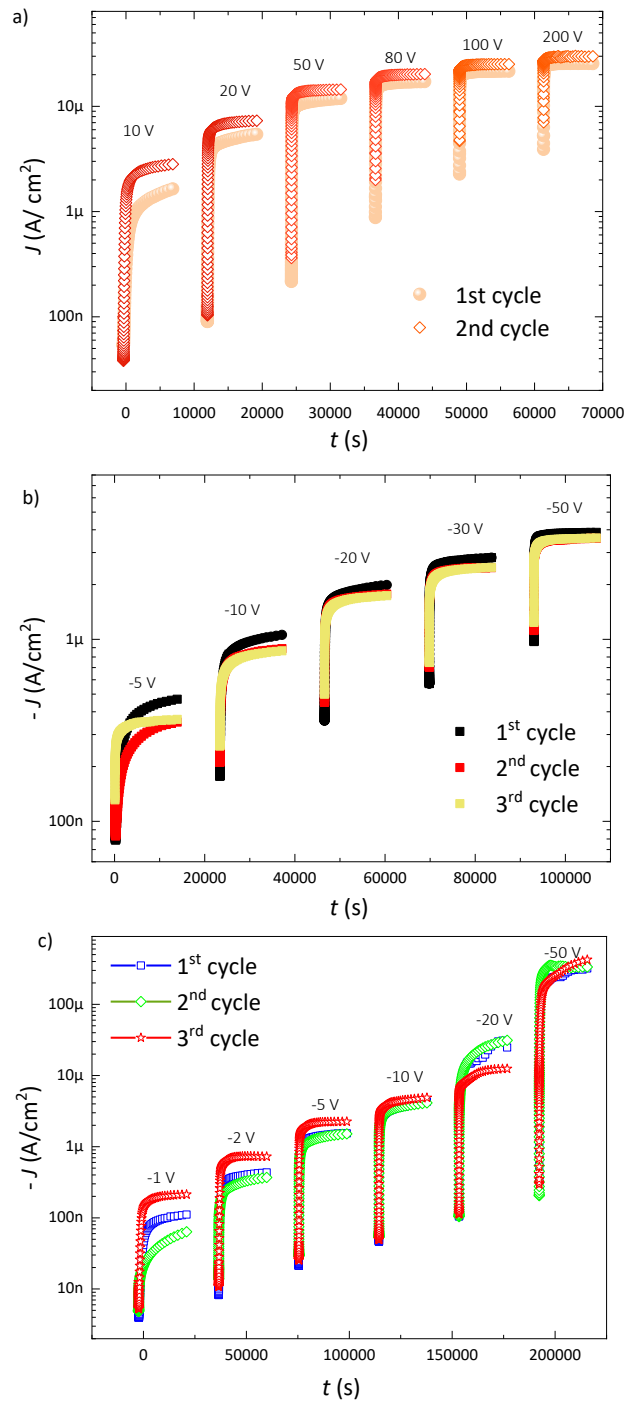


Figure S2. Protocol of measurement based on long-time current transient's response to different voltage steps of a) a 2.2 mm MAPbBr_3 SC- symmetrically contacted with evaporated Cr electrodes and two samples of b) MAPbBr_3 MC and c) MAPbI_3 MC contacted with Pt/Cr electrodes. Note the reproducibility between cycles.

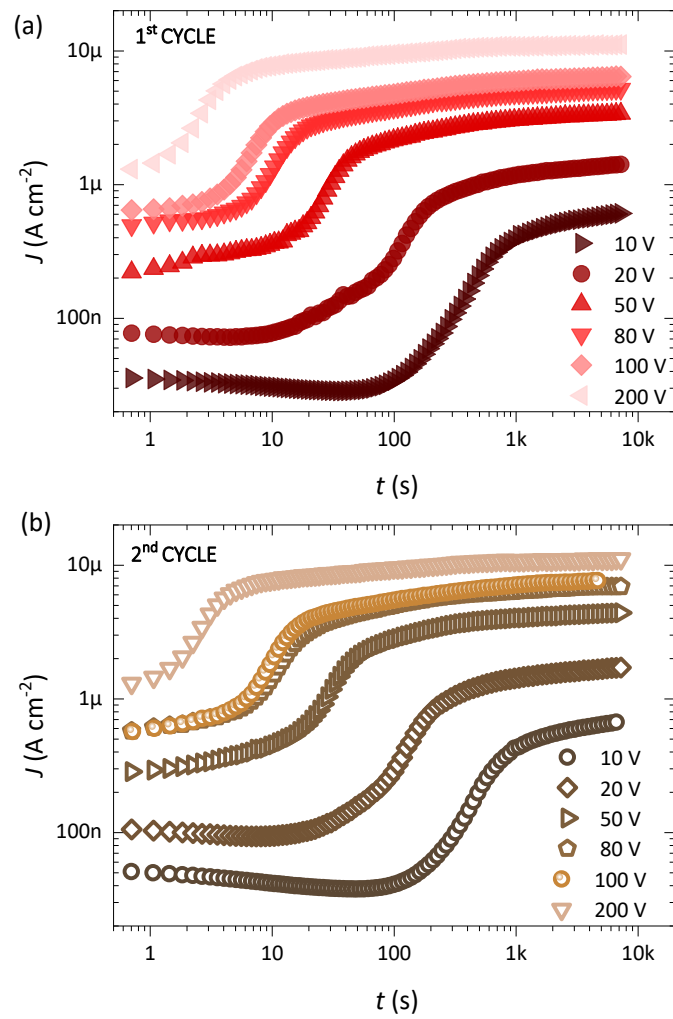


Figure S3. Long-time current transient response to different voltage steps during the 1st and b) 2nd cycle of measurement of a 2 mm-thick MAPbBr₃ SC.

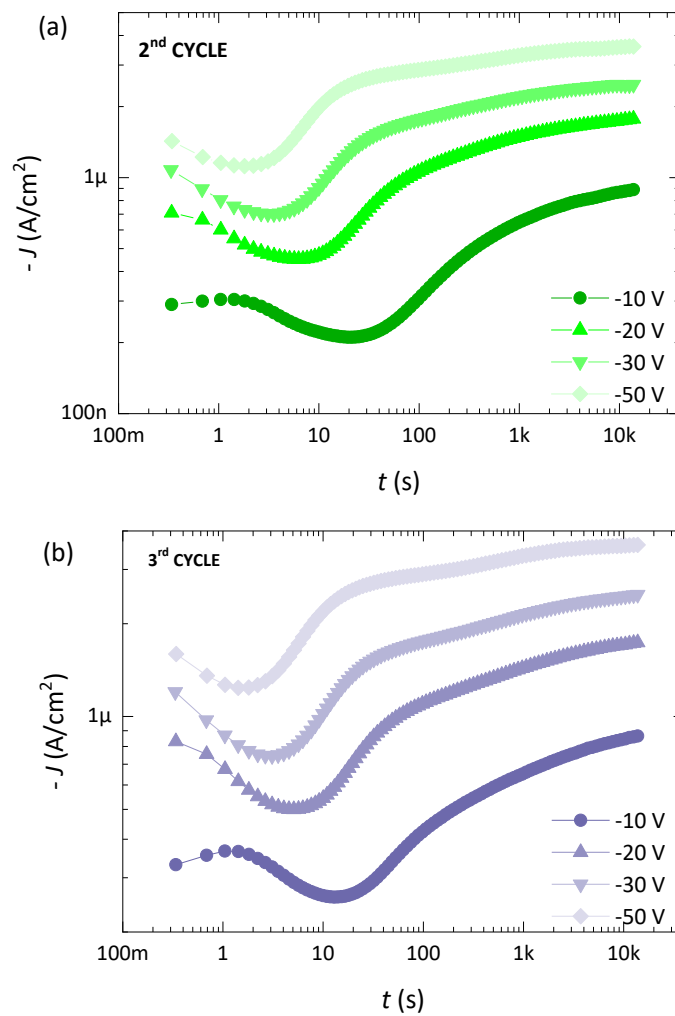


Figure S4. Long-time current transient response to different voltage steps during the 2nd and b) 3rd cycle of measurement of a 1.5 mm-thick MAPbBr₃ MC.

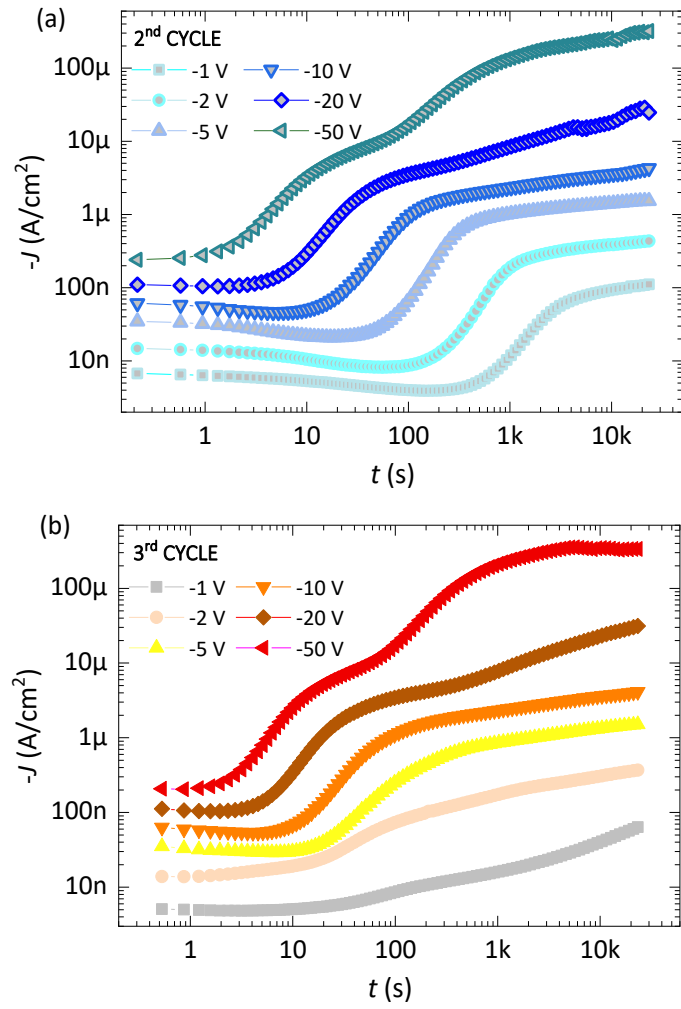


Figure S5. Long-time current transient response to different voltage steps during the 2nd and b) 3rd cycle of measurement of a 1 mm-thick MAPbI₃ MC.

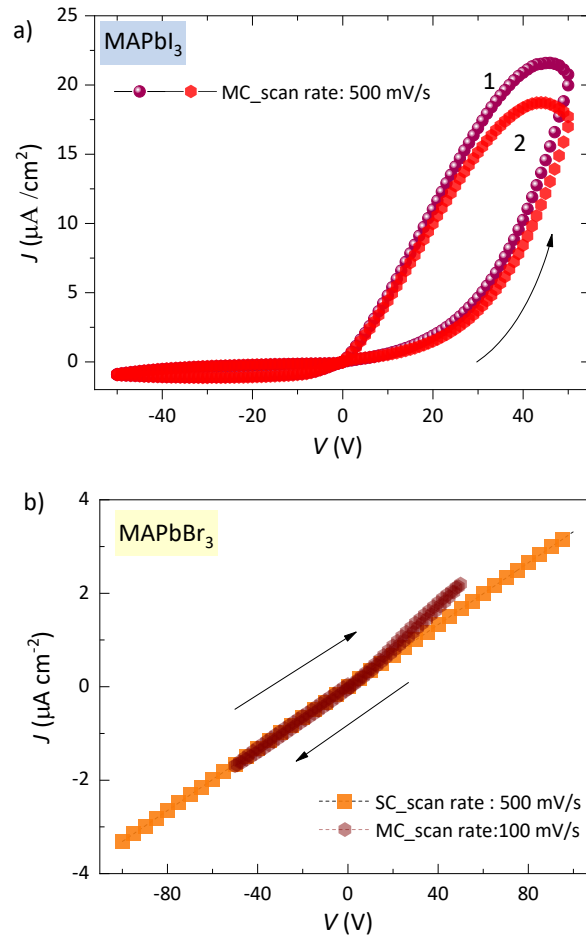


Figure S6. Current–voltage characteristics (j - V) with scan rate of a) 500 mV/s and step of 1 V of 1 mm-thick MAPbI₃ MC sample b) 500 mV/s and 100 mV/s and step of 1 V of firstly, a 2 mm-thick MAPbBr₃ SC and secondly a 1.5 mm-thick MAPbBr₃ MC. In Fig b it is remarkable the ohmic character of the characteristics j - V curve, in agreement with previous analysis on Cr-contacted perovskite device¹

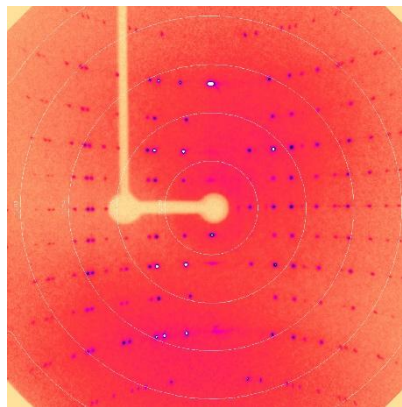


Figure S7. Rotation XRD spectra along α cell axis of a crystal measured with Cu radiation. In here only dots appear and the absence of concentric circles supports the

monocrystalline nature of the crystal. However, is evident the high symmetry observed in the material around one axis

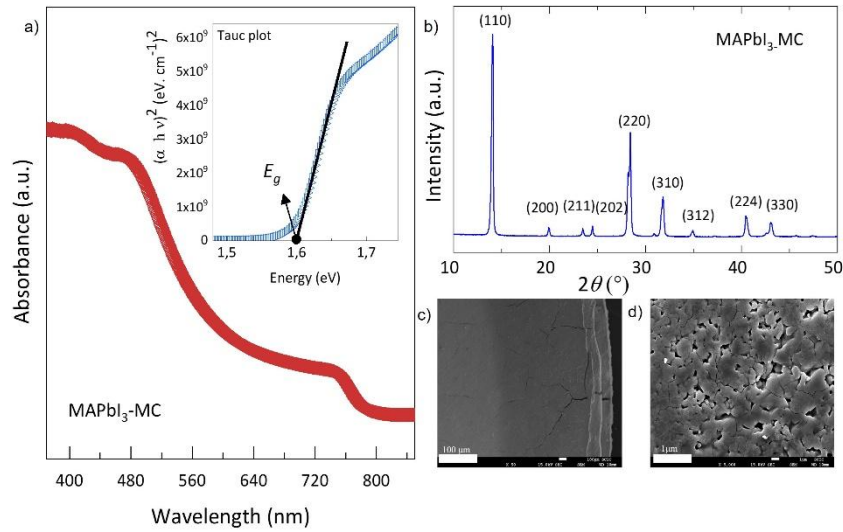


Figure S8. a) Absorbance spectra of MAPbI₃ MC sample Inset: Tauc-plot of the pellet (thickness ~1000 μm), showing the typical absorption edge of MAPbI₃ in 1.60 eV b) PXRD pattern of MAPbI₃-MC sample confirming a single-phase sample with tetragonal symmetry at room temperature. The film show the (110), (220), and (310) peaks at 14.1°, 28.4°, and 32.1°, respectively. These values are in good agreement with the reported values²⁻³ c) and d) SEM images of the top view of a MAPbI₃ thick pellets showing the microcrystalline nature of the sample at different magnified areas.

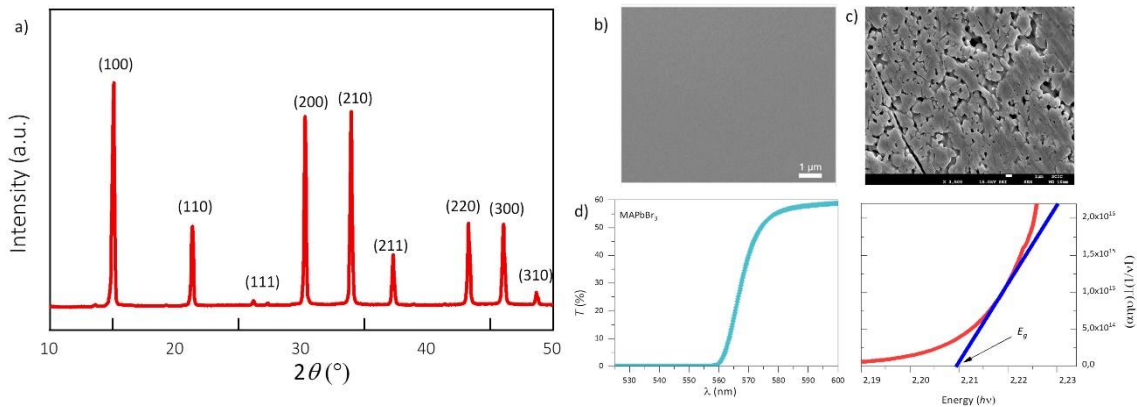


Figure S9. a) Image of the PXRD diffractogram of MAPbBr₃-MC sample showing cubic crystal lattice (Pm3m space group). The diffractogram show the (100), (110), and (200) (210) peaks at 15.0°, 21.21°, and 30.12 ° and 33.78 ° respectively. These values agree with those found in the literature.⁴⁻⁶ SEM images of the top view of a b) of MAPbBr₃-SC sample after a polishing procedure and a c) of MAPbBr₃-MC sample

showing a different surface morphology d) Transmittance spectra of MAPbBr₃-SC via UV-visible spectroscopy (SC thickness = 2.0 mm) In the inset: Tauc plot of MAPbBr₃-SC for band gap determination ($E_g = 2.18$ eV)

1. García-Batlle, M.; Baussens, O.; Amari, S.; Zaccaro, J.; Gros-Daillon, E.; Verilhac, J. M.; Guerrero, A.; Garcia-Belmonte, G., Moving Ions Vary Electronic Conductivity in Lead Bromide Perovskite Single Crystals through Dynamic Doping. *Adv. Electron. Mater.* **2020**, *6*, 2000485.
2. Aranda, C.; Cristobal, C.; Shooshtari, L.; Li, C.; Huettnner, S.; Guerrero, A., Formation Criteria of High Efficiency Perovskite Solar Cells under Ambient Conditions. *Sustainable Energy Fuels* **2017**, *1*, 540-547.
3. Alias, M. S.; Dursun, I.; Saidaminov, M. I.; Diallo, E. M.; Mishra, P.; Ng, T. K.; Bakr, O. M.; Ooi, B. S., Optical Constants of CH₃NH₃PbBr₃ Perovskite Thin Films Measured by Spectroscopic Ellipsometry. *Opt. Express* **2016**, *24*, 16586-16594.
4. Amari, S.; Verilhac, J.-M.; Gros D'Aillon, E.; Ibanez, A.; Zaccaro, J., Optimization of the Growth Conditions for High Quality CH₃NH₃PbBr₃ Hybrid Perovskite Single Crystals. *Cryst. Growth Des.* **2020**, *20*, 1665-1672.
5. Murali, B.; Kolli, H. K.; Yin, J.; Ketavath, R.; Bakr, O. M.; Mohammed, O. F., Single Crystals: The Next Big Wave of Perovskite Optoelectronics. *ACS Mater. Lett.* **2020**, *2*, 184-214.
6. Saidaminov, M. I., et al., High-Quality Bulk Hybrid Perovskite Single Crystals within Minutes by Inverse Temperature Crystallization. *Nat. Commun.* **2015**, *6*, 7586.